Journal of Engineering Technology (ISSN: 0747-9964)
Volume 6, Issue 2, July, 2017, PP.216-231

ORIGINAL ARTICLE

Analysis of stability in turning with secondary effects

B .Tulasiramarao[*1], K.srinivas[2], P. Ram Reddy[3]

[1]Research Scholar, Dept of Mech Engg. JNTU Hyderabad, Telangana, India
[2]Professor, Dept of Mech Engg. RVR&JC college of Engineering, Guntur, AP, India
[3] Professor, Dept of Mech Engg. & Former Registrar, JNTU Hyderabad, Telangana, India.

Abstract: This paper proposes an analytical scheme for stability analysis in turning process by considering the motion of tailstock-supported workpiece using a compliance model of tool and work. It explains the effect of secondary parameters like workpiece dimensions, cutter position and dynamic nature of the system. A dynamic cutting force model based on relative motion between the cutting tool and workpiece is developed to study the chatter stability. Linear stability analysis is carried out in the frequency domain and the stability charts are obtained with and without considering workpiece flexibility. Variations of stability limits with workpiece dimensions and cutter position as well as the effects of cutting tool dynamics are studied and wherever possible results are compared with existing models. Experimental analysis is conducted on tailstock-supported workpiece to examine the correctness of the proposed stability model.
Keywords: Chatter stability, Regeneration, Compliance, Two-degree model, Critical parameters

1. Introduction

Many engineering components manufactured using casting, forming and other processes often require machining as their end operation. Machining or metal cutting is an important manufacturing process. With the modern trend of machine tool development, accuracy and reliability are becoming prominent features. To achieve higher accuracy and productivity, it requires consideration of dynamic instability of cutting process. When there is a relative motion present between the tool and work piece, the performance of the operations may not be satisfactory. The machine tool vibrations have detrimental effect on tool life which in turn lowers the productivity and increases cost of production. The process of cutting in turning exhibits complicated and interesting dynamics. During the cutting operation, several types of vibrations influence the chip flow-rate and final work surface. Compared to free and forced vibrations, self-excited vibrations are more detrimental to the finished surfaces and cutting tools. Self-excited vibrations are developed at one of the natural modes of cutting system as a result of dynamic interaction between the structure and cutting process. This may result in large amplitudes of relative motion between the cutter and work-piece. Such a phenomenon also known as ‘chatter’ can in general result from one or more of the following: regenerative effects, mode coupling, loss-of-contact dynamics, and friction, structural and other sources of nonlinearities. Of all these, regenerative chatter has more influence on the stability of cutting. The regeneration is due to interaction of cutting force and work-piece surface undulations reduced by the preceding tool passes. It occurs when the cuts overlap and cut produced at a time t leaves small waves in the material that are regenerated during each subsequent pass of the tool. If regenerative vibrations becomes large enough so that the tool does not be in contact with work-piece, another type of chatter known as multiple regenerative chatter occurs. Machine tool can vibrate due to cutting process itself under some particular conditions. The excitation is supplied by the cutting process itself. Boothroyd & Knight[1] and Astkhov[2] stated that machine tool vibrations may be divided into the three types i.e. free vibration, forced vibration, and self-excited vibration. These authors defined self excited

vibrations as free vibrations with negative damping. In the middle of the twentieth century, Arnold[3] demonstrated the negative damping effect using his experimental studies and analytical modeling. Andrew & Tobias[4] discussed and compared two current theories of machine tool chatter considering differences in their basic assumptions and their theoretical structure. Gurney & Tobias[5] found that the regeneration is due to variations in the uncut chip thickness from one revolution to another. They presented a method of analysis of machine tool stability during turning operation.Tlusty & Polacek[6] presented the stability of machine tool against self-excited vibration in turning operation with and without coolants. Tlusty[7] presented a method to analyse the stability of the machine tool in turning operation and explained about the various cutting parameters and its effect on stability. Tobias, and Fishwick[8] explained the structural dynamics of the machine tool and the feedback between the subsequent cuts on the same cutting surface, and thus modulation in the chip thickness. Tarng *et al.*[9] presented another analytical model of chatter vibration in metal cutting. The basic cutting mechanics adopted in this model is derived from a predictive machining theory based on a shear zone model of chip formation. In this model the variation of undeformed chip thickness and rake angle due to the machine tool vibration are measured. Altintas and Weck[10] presented orthogonal chatter stability law and lobe diagrams for single point machining operations where the process is one dimensional and time invariant. Here various stability models are compared against experimentally validated time domain simulation model results. Chen and Tsao[11] analyzed the stability of the cutting system in terms of the work-piece length, radius, natural frequency, deflection, slenderness ratio, cutting point, and material. The relationship between the critical chip width and the cutter spindle speed is investigated under a range of cutting and work-piece conditions. The analytical results for the flexible work-piece are compared with those for a rigid work-piece. It is found that the critical chip width of the flexible work-piece is always greater than that of the rigid body. Ganguli *et al.*[12] demonstrated the effect of active damping on regenerative chatter instability for a turning operation. Here an active damping is proposed as a strategy to enhance the stability limits of the system. It is shown that different spindle speeds cause changes in the system damping, resulting in different levels of stability limits at different spindle speeds. Practically, the regeneration is a nonlinear phenomenon. The various forms of nonlinearity are considered in the analytical models. The popular way is to treat the cutting force as a nonlinear function of time varying chip width or feed. This nonlinear force-feed relation leads to a different stability states. Most nonlinear chatter models consider either nonlinearity in the structure and cutting force or nonlinearity due to friction depending on the cutting speed. Insperger *et al.*[13] analysed non-linear dynamics of a state-dependent delay model of the turning process. The size of the regenerative delay is determined not only by the rotation of the workpiece, but also by the vibrations of the tool. The numerical analysis of their model revealed that Hopf bifurcations depend on the feed rate. Landers and Ulsoy[14] presented a nonlinear force feed model to illustrate the practical machining simulations in turning and milling operations. Here machining chatter analysis techniques are mainly examine the stability of the closed-loop model of the machining operation to determine the stable process parameter space. In metal removal operations, much of the research work has been carried out in the past and many are continuing for the purpose of decreasing production cost and to increase the product quality. Thomas *et al.* [15] had shown the effect of tool vibration on surface roughness during dry turning at different cutting parameters and tool angles.

2. Analytical models

Stability lobe diagrams indicate the critical operating parameters necessary to avoid unstable cutting conditions. For every cutting operation, there is one such diagram which takes into account several features such as varying tool wear, work-piece supporting conditions, range of operating speeds, tool overhang lengths and so on. To draw the stability-lobe diagram involving many cutting states, it is quite tedious to perform the

experiments several times. Analytical models on the other hand help to obtain the status of stability by incorporating several features in dynamic equations. However, care should be taken during modeling to incorporate all practical cutting constraints to maximum possible extent.

2.1 Compliant Dynamic Model of Cutting Tool and Workpiece

The dynamic stability of a machine tool in the turning process depends essentially on the compliance of the lathe structure, as well as on the properties of the cutting process. However, the design of the machine tool, the material(s) employed for its manufacture and their mechanical properties are extremely important for the dynamic behaviour of the machining system (comprising the entire lathe and the work material). The main input parameters affecting the machining system vibrations are: work material, work material geometry, tool material, tool geometry, lathe rigidity, cutting conditions (cutting speed, feed rate, and depth of cut) and tool wear. The behaviour of the machining system during vibration is a major output parameter.

Basically, the turning tool is represented with a single degree for freedom spring-mass system working over a rigid workpiece. Cutting parameters such as cutting speed, feed, depth of cut, and tool overhang length have been accounted in the models to understand their effects on chatter stability in terms of critical chatter length. Different models are presented in the literature for development of analytical techniques for stability analysis. In the first case, the stability analysis in turning process is presented with a compliant dynamic model of cutting tool and workpiece. Effect of cutting tool position, workpiece dimensions, tool stiffness and damping on the dynamic stability is presented with the proposed dynamic model. Tool and workpiece are modeled as two separate single degree of freedom spring-mass damper systems. The model allows selection of different operating conditions with and without a tailstock support by accounting the fundamental natural frequency of the workpiece. Overall transfer matrix is derived from the equations of motion in the Laplacian domain and the expressions for critical parameters of cutting process in stable conditions are obtained analytically. Effect of workpiece parameters such as linear and lateral dimensions and cutter positions as well as influence of flexibility and damping of cutter on the stability is studied. In verifying the proposed model, experimental analysis is conducted on an engine lathe with a tail stock-supported AISI 1045 steel workpieces under various operating conditions. Dynamic cutting forces are recorded with a lathe tool dynamometer.

2.2 Dynamic modeling

In most of the turning operations, workpiece is considered as a rigid member and the chip thickness is assumed to be affected only by the dynamic parameters of cutting tool. This one-dimensional second order orthogonal cutting model shown in Figure.1 is represented with the following governing equation:

$$m_1\ddot{x}(t)+c_1\dot{x}(t)+k_1x(t)=F(t)\cos\theta t \quad (1)$$

Here, x(t) is chip thickness (variation in depth of cut) at a time t and the parameters m_1,c_1 and k_1 are the equivalent mass, damping, and stiffness of the cutting tool and tool holder, θ is a constant cutting angle and F(t) is cutting force, which is given by:

$$F(t)=Cbh(t) \quad (2)$$

Where C is cutting coefficient obtained from experiments and b is depth of cut or chip width. The instantaneous chip thickness h(t) can be written from Figure 1 as:

$$h(t)= h_0-x(t)+x(t-\tau) \quad (3)$$

here, x (t−τ) is chip thickness in previous cut ; h_0 is nominal chip thickness resulting from feed mechanism and the term x(t)−x(t−τ) represents the regenerative chatter. Time delay τ represents the period for successive passages of tool, which is equal to time required for one revolution of workpiece in turning.

Journal of Engineering Technology (ISSN: 0747-9964)
Volume 6, Issue 2, July, 2017, PP.216-231
ORIGINAL ARTICLE

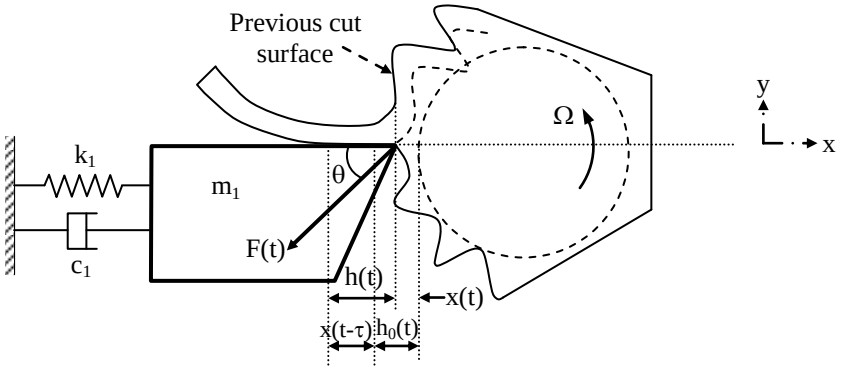

Fig.1 Cutting tool model with rigid workpiece

Substituting Eqs.(2) and (3) in Eq.(1) and taking Laplace transforms on both sides, the dynamic equation in Laplacian(s) domain becomes:

$$(m_1 s^2 + c_1 s + k_1)X(s) = Cb(H_0(s) - X(s) + e^{-s\tau}X(s)) \quad (4)$$

Thus the overall transfer function becomes

$$\frac{X(s)}{H_0(s)} = \frac{bCG(s)}{1 + bCG(s)(1 - e^{-s\tau})} \quad (5)$$

where $$G(s) = \frac{\cos\theta}{m_1 s^2 + c_1 s + k_1} \quad (6)$$

In practice, operating spindle speeds are well below the natural frequency of workpiece. Hence, in the flexibility considerations, the first mode of vibration is considered as significant and the workpiece is represented as another single degree of freedom spring mass damper system as shown in Figure 2.

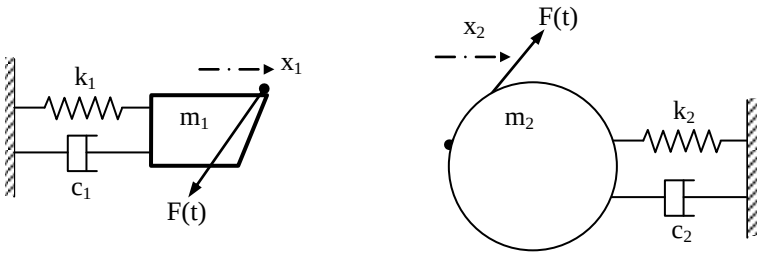

(a) model of cutting tool (b) model of workpiece

Fig.2 Proposed Compliant Model

For this combined system, the equations of motion can be written in terms of tool and workpiece deformations $x_1(t)$ and $x_2(t)$ at a time t as follows:

$$m_1 \ddot{x}_1(t) + c_1 \dot{x}_1(t) + k_1 x_1(t) = -F(t)\cos\theta \quad (7)$$

$$m_2 \ddot{x}_2(t) + c_2 \dot{x}_2(t) + k_2 x_2(t) = F(t)\cos\theta \quad (8)$$

Here m_2, c_2, and k_2 respectively represent mass, damping coefficient, and stiffness of the workpiece. F(t) is dynamic feed force which can be expressed in terms of the present and previous relative motion of cutting tool with respect to work-piece: $(x_1(t) - x_2(t))$ and $(x_1(t - \tau) - x_2(t - \tau))$. That is force

Journal of Engineering Technology (ISSN: 0747-9964)
Volume 6, Issue 2, July, 2017, PP.216-231
ORIGINAL ARTICLE

$$F(t) = Cb\{h_0 - (x_1(t) - x_2(t)) + (x_1(t-\tau) - x_2(t-\tau))\} \quad (9)$$

When the above force term F(t) in Eq.(9) is substituted in Eqs.(7) and (8) and writing $k_1/m_1 = \omega^2_{n1}$, $k_2/m_2 = \omega^2_{n2}$, $c_1/m_1 = 2\xi_1\,\omega_{n1}$, $c_2/m_2 = 2\xi_2\,\omega_{n2}$, these two equations become coupled dynamic equations in terms of the variables x_1 and x_2 as follows.

$$\ddot{x}_1(t) + 2\xi_1\omega_{n1}\dot{x}_1(t) + \omega^2_{n1}x_1(t) = -\frac{Cb\cos\theta}{m_1}\{h_0 - (x_1(t) - x_2(t)) + (x_1(t-\tau) - x_2(t-\tau))\} \quad (10)$$

$$\ddot{x}_2(t) + 2\xi_2\omega_{n2}\dot{x}_2(t) + \omega^2_{n2}x_2(t) = -\frac{Cb\cos\theta}{m_2}\{h_0 - (x_1(t) - x_2(t)) + (x_1(t-\tau) - x_2(t-\tau))\} \quad (11)$$

Here ω_{n1},ω_{n2} and ξ_1,ξ_2 are natural frequencies and damping ratios of the cutter and work piece, respectively.

In Laplacian domain, Esq.(10) and (11) can be written as :

$$s^2X_1(s) + 2\xi_1\omega_{n1}sX_1(s) + \omega^2_{n1}X_1(s) = -\frac{Cb\cos\theta}{m_1}\{H_0(s) - (1 - e^{-\tau s})X_1(s) + (1 - e^{-\tau s})X_2(s)\} \quad (12)$$

$$s^2X_2(s) + 2\xi_2\omega_{n2}sX_2(s) + \omega^2_{n2}X_2(s) = \frac{Cb\cos\theta}{m_2}\{H_0(s) - (1 - e^{-\tau s})X_1(s) + (1 - e^{-\tau s})X_2(s)\} \quad (13)$$

These can be simplified and a vector of transfer functions can be written of the form:

$$\frac{X(s)}{H_0(s)} = [A]^{-1}\{B\} \quad (14)$$

where $$X(s) = \begin{Bmatrix} X_1(s) \\ X_2(s) \end{Bmatrix} \quad (15)$$

$$[A] = \begin{bmatrix} \phi_1 + pm_2(1 - e^{-\tau s}) & -pm_2(1 - e^{-\tau s}) \\ -pm_2(1 - e^{-\tau s}) & \phi_2 + pm_1(1 - e^{-\tau s}) \end{bmatrix} \quad (16)$$

$$\{B\} = \begin{Bmatrix} -pm_2 \\ pm_1 \end{Bmatrix} \quad (17)$$

and $$p = \frac{Cb\cos\theta}{m_1m_2} \quad (18)$$

The functions $\phi_1 = (s^2 + 2\xi_1\omega_{n1} + \omega^2_{n1})$ and $\phi_2 = (s^2 + 2\xi_2\omega_{n2} + \omega^2_{n2})$ are defined for convenience.

2.3 Stability analysis

The stability can be analyzed by considering the characteristic equation of the system and studying the relationship between the spindle speed N and chip width b.

For rigid work-piece analysis from Eq.(5) the characteristic equation is obtained by equating denominator to zero. That is :

$$1 + bC\frac{(1e^{-\tau s})\cos\theta}{m_1s^2 + c_1s + k_1} = 0 \quad (19)$$

Journal of Engineering Technology (ISSN: 0747-9964)
Volume 6, Issue 2, July, 2017, PP.216-231
ORIGINAL ARTICLE

Substituting s = jω, separating real and imaginary terms, and solving for τ and b yields the following critical values:

$$\tau^* = \frac{2}{\omega}\left\{(n+1/2)\pi + a\tan\left[\frac{c_1\omega}{m_1\omega^2 - k_1}\right]\right\} \quad (20)$$

where n = 0,1,2…….

$$b^* = -\frac{c_1\omega}{C\cos\theta\sin\omega\tau^*} \quad (21)$$

Here ω is the chatter frequency. Spindle speed in revolution per second is computed as $N = 1/\tau^*$. It can be seen that Eq.(20) has multiple solutions due to different values of n. Thus, Esq. (20) and (21) define the stability limits of this system.

In the case of compliant model development the stiffness of work-piece has to be defined in terms of cutter location and supporting length. In turning operation, the cutting is often performed with and without tailstock supports. As shown in Fig.3(a), when there is no tailstock support for workpiece, it can be treated as a cantilever beam of stiffness $k_2 = \frac{3EI}{L^3}$. Here I and L are the moment of inertia and overhang length of work-piece respectively. E is Young's modulus of work-piece material. While modeling, the tailstock supported work-piece, the work can be considered as propped cantilever beam as shown in Fig.3(b). When cutting is performed at any location L_1 on a tailstock-supported workpiece, the corresponding cutting force causes the workpiece to deflect. The maximum deflection in between the supports defines the stiffness of the is accounted as stiffness of workpiece in the proposed model. Thus

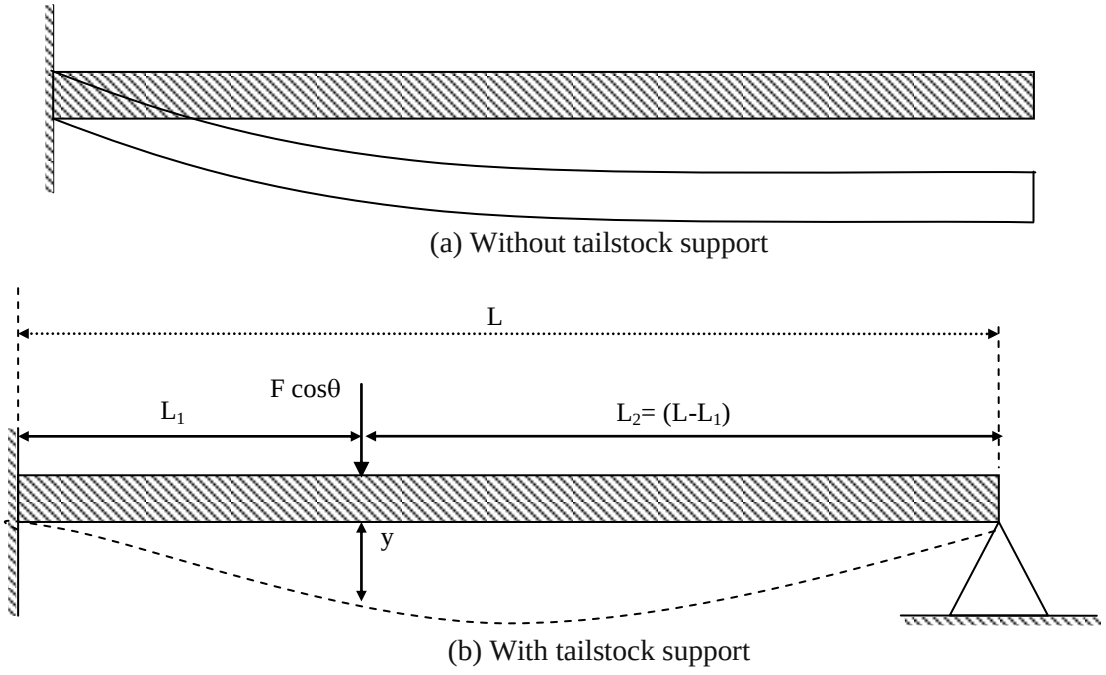

(a) Without tailstock support

(b) With tailstock support

Fig.3 Deflection of tailstock-supported workpiece

Using the expression for stiffness of propped-cantilever beam:

$$k_2 = \frac{-12L^3EI}{L_1^2L_2\{3L(L_2^2 - L^2) + L_1(3L^2 - L_2^2)\}} \quad (22)$$

Journal of Engineering Technology (ISSN: 0747-9964)
Volume 6, Issue 2, July, 2017, PP.216-231
ORIGINAL ARTICLE

The fundamental natural frequency of workpiece: $\omega_{n2}=\sqrt{\frac{k_2}{\rho AL}}$ is obtained. Here, ρ is material density; L is total length between the supports and A is the cross-sectional area of workpiece. From Eqs. (14), (15), (16), (17) and (18), the characteristic equation for flexible model can be expressed as:

$$\phi_1\phi_2 + p(1-e^{-\tau s})(\phi_1 m_1 + \phi_2 m_2) = 0 \quad (23)$$

Substituting s = jω and expanding Eq. (23) and separating real and imaginary terms, it result in:

$$(a_1a_2 - b_1b_2) + p\{(1-\cos\omega\tau)A - B\sin\omega\tau\} = 0 \quad (24)$$

$$(a_1b_2 - a_2b_1) + p\{(1-\cos\omega\tau)B + A\sin\omega\tau\} = 0 \quad (25)$$

where $a_1 = (\omega_{n1}^2 - \omega^2), b_1 = 2\xi_1\omega_{n1}\omega, a_2 = (\omega_{n2}^2 - \omega^2), b_2 = \xi_2\omega_{n2}\omega,$

$A = (m_1a_1 + m_2a_2), B = (m_1b_1 + m_2b_2)$

Eliminating p from Esq. (24) and (25) and defining D = (a_1a_2 – b_1b_2) and E = (a_1b_2 – a_2b_1), the phase shift can be written as :

$$\tan\psi = -\frac{\sin\omega\tau}{1-\cos\omega\tau} = \frac{-1}{\tan\frac{\omega\tau}{2}} = \tan\left(\frac{\omega\tau}{2} - \frac{\pi}{2} - n\pi\right) = \frac{BD - AE}{AD + BE} \quad (26)$$

This equation gives the critical time τ^* as:

$$\frac{\omega\tau^*}{2} = \left\{\left(n + \frac{1}{2}\right)\pi + a\tan\left[\frac{BD - AE}{AD + BE}\right]\right\} \quad (27)$$

where n = 0, 1, 2, ….

Also the critical chip width is:

$$b^* = \frac{m_1m_2}{C\cos\theta}\left[\frac{D}{B\sin\omega\tau - A(1-\cos\omega\tau^*)}\right] \quad (28)$$

The equations (27) and (28) define the stability limits for a cutting tool and work-piece. Thus the dynamic characteristics of work-piece and cutting tool are used to obtain the stability lobe diagram.

3. Experimental analysis

In order to verify the analytical models, several tests are conducted to collect the required data through measurements which are done before, during and after the cutting tests. In the first two cases of experiments dynamic cutting forces are only measured in order to know the effects of workpiece flexibility and nonlinear force feed respectively on the cutting stability. In the third case, influence of secondary parameters like tool overhang length and flank wear on the cutting dynamics are studied by measuring the static cutting force data, workpiece surface roughness, tool wear as well as critical chatter lengths. In machining practice cutting force signals carry good amount of information regarding dynamics of cutting. When stability is lost, the feedback between the displacement and cutting forces begins, which results in an erratic cutting force histories. These cutting force histories are often recorded by means of lab-view equipped tool post dynamometers. Fig.4 illustrates the arrangement for dynamic cutting force measurement using lathe tool-dynamometer.

Journal of Engineering Technology (ISSN: 0747-9964)
Volume 6, Issue 2, July, 2017, PP.216-231

ORIGINAL ARTICLE

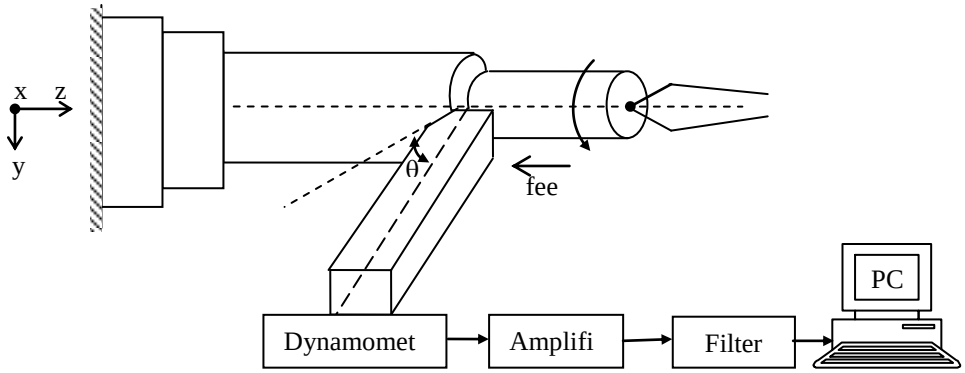

Fig.4 Arrangement for dynamic force measurement

For testing the effects of work flexibility and compliance between work and tool, a series of cutting experiments are conducted on a 7.5 KW engine lathe with tailstock supported work-pieces. The cutting tools are carbide inserts and cutting is performed orthogonally. Work material is AISI 1045 steel. The cutting variables like depth of cut and spindle RPM are varied and cutting force histories are obtained. The major cutting conditions employed are depicted in Table 1.

Table.1 Major cutting conditions in experiment-1

Feed(mm/rev)	0.246
Depth of cut (mm)	1.47, 1.525, 1.58
Spindle speed(RPM)	110, 550, 770

Feed is adjusted with auto setting; depth of cut is measured and given by a dial gauge, while spindle speeds are selected by changing lever positions according to the manufacturer's tables. In order to measure output forces Kistler-9121 three-component piezoelectric dynamometer is employed. There is an associated 5070 multi-channel charge amplifier connected to PC employing Kistler Dynoware force measurement post processing software. The cutting force measurements in each case are made over a specified time span. Computer incorporating menu driven Dynoware software continuously plots cutting forces in X, Y and Z directions over the time span. User can vary the sampling frequency rate. The measured cutting forces are digitized and saved in the post processor files. This time domain data can be translated into a text file and time histories are drawn using EXCEL or MATLAB so as to obtain the corresponding FFT spectrums. Prior to the cutting force measurements, modal data of cutting tool and work-piece are obtained from impact hammer testing, as the natural frequencies and damping ratios of work-piece and tool are required first. Then stiffness of tool and work-piece are also measured on the same set-up by measurement of amplitude of deflection for given amplitude of tip impact hammer excitation. Work-pieces of 60 mm diameter and set-over length of 250 mm are used under various operating conditions. Fig.5 shows the experimental set-up used for measurement of modal parameters along with the dynamometer arrangement.

Journal of Engineering Technology (ISSN: 0747-9964)
Volume 6, Issue 2, July, 2017, PP.216-231

ORIGINAL ARTICLE

Fig.5 Experimental set-up for finding modal data

The impact hammer contains a quartz force sensor mounted on the striking tip of the hammer head. That quartz force sensor is used to transfer impact force into electrical signal for display and analysis. Signals generated by impact hammer and the accelerometer are traced in the signal analyzer using amplifiers. In the present task, Kistler 9724A impact hammer is used to excite the work-piece and cutting tool. To measure the vibratory response, small piezoelectric accelerometers (model Kistler 8632C50) are mounted in two lateral directions of workpiece. Here 5134A microprocessor-controlled coupler provides power and signal processing.

4. Results and discussion

This section presents the results of various analytical models proposed in the work along with the experimental validations wherever necessary. Initially, the output stability results of multi-degree of freedom tool and work compliance model are described. The second model comprising of nonlinear force-feed effect is illustrated with an oblique cutting process. Both the stability lobe diagrams and time-domain solutions are obtained from the model. Finally the results of experiments carried-out in knowing the influence of secondary parameters such as tool overhang on the output parameters like cutting forces are presented for four different work materials. These experimental results are employed further to develop a cutting model using radial basis neural networks. Finally the optimization results of cutting process are derived from this neural network model using binary coded genetic algorithms. Results are shown in the form of graphs and tables.

4.1 Compliance between Cutting Tool and Work

The analytical model described earlier is used to draw the stability lobe diagram under some preset conditions. That is the omega value is varied from a minimum value to a maximum in each lobe. Each such lobe forms the part of the entire lobe diagram. Initially, when the work-piece is rigid, the standard lobe diagram is obtained. The cutting tool and work-piece data selected from Chen and Tsao work is shown in Table 2.

Table 2. Cutting tool and work-piece data [25]

Component / parameter	Tool	Work-piece(steel)
m (kg)	50	--
c (kg/s)	2×10^{3}	--
K (N/m)	2×10^{7}	--
C (N/m^2)	2×10^{9}	--

Journal of Engineering Technology (ISSN: 0747-9964)
Volume 6, Issue 2, July, 2017, PP.216-231
ORIGINAL ARTICLE

Θ	70^o	--
E (Gpa)	--	180
ρ (kg/m^3)	--	7850
L (m)	--	0.25, 0.5
r (m)	--	0.025, 0.03, 0.035, 0.04, 0.05

4.2 Effect of work-piece dynamics

When cutting force deflects the work-piece, the effect of work deflections on stability of cutting process are shown in Figure 6.

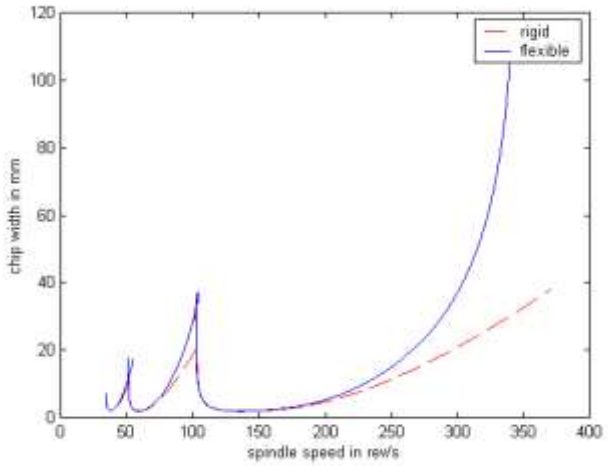

Fig.6 Comparative lobe diagram for rigid and flexible work-pieces
(r = 0.03 m, L = 0.3 m and L_1 = 0.6L)

This figure shows the relationship between the critical chip width and the spindle speeds for work-pieces of length 0.5 m and radius 0.03 m. For comparison purpose, the results for both the rigid (dashed line) and flexible work-piece cases (solid line) are presented. It is seen that critical chip-width at higher spindle speeds is considerably larger when the work-flexibility is considered. The results reveal that for a constant spindle speed, the critical chip width is consistently higher when the work-piece deformation is taken into consideration. Figure 7 shows the variation of percentage difference of chip-width in both cases as a function of spindle speed. It can be seen that maximum percentage deviations are noticed at the right side of the diagram. This diagram is very much coinciding with the published work, where the authors considered the work-piece as a continuous cantilever beam simply supported at the free end.

Journal of Engineering Technology (ISSN: 0747-9964)
Volume 6, Issue 2, July, 2017, PP.216-231

ORIGINAL ARTICLE

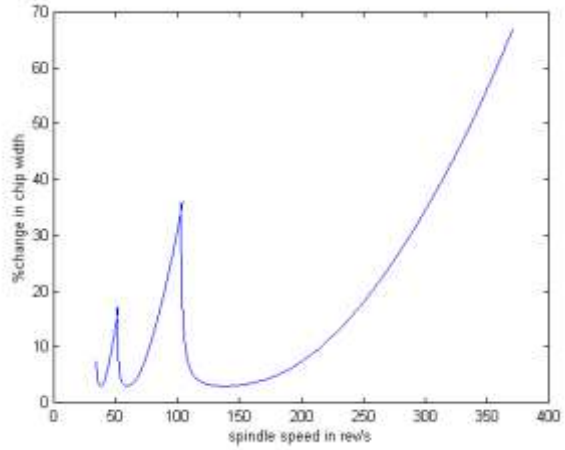

Fig.7 Percentile difference of chip-width verses speed between rigid and flexible work-piece models

Figure 8 shows variation of percentage difference in the critical chip-width as a function of spindle speed for four different work-pieces of constant length 0.5 m with different radii. A single lobe at higher speeds is only shown for clarity. As noticed from earlier works, here also the percentage difference of chip-width decreases progressively with increase in radius.

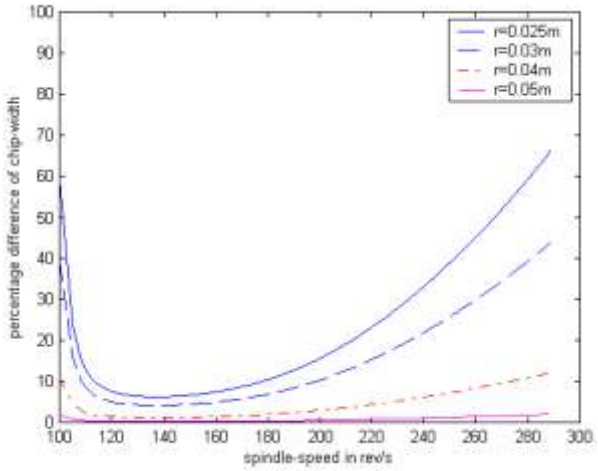

Fig.8 Variation of percentage difference in chip-width (L = 0.5m) as a function of radius

Figure 9 shows the variation of percentage difference in critical chip-width as a function of spindle speed for two work-pieces of constant radius 0.03 m, with two different lengths.

Journal of Engineering Technology (ISSN: 0747-9964)
Volume 6, Issue 2, July, 2017, PP.216-231

ORIGINAL ARTICLE

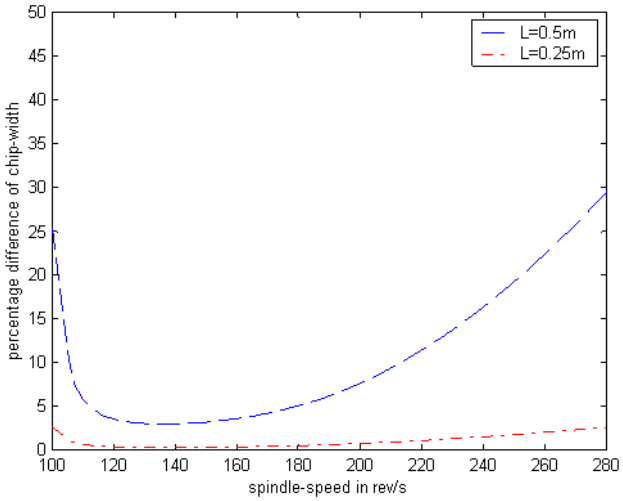

Fig.9 Percentage difference in chip-width versus speed for Work-piece of constant radius (r = 0.03m)

From the diagram it can be observed that larger work-piece has more deflection and critical chip-width. In all the above cases, the position of cutting tool is considered at L_1=0.6L. The damping ratio for all work-piece conditions is taken as 0.025, since it normally varies from 0.01 to 0.05. Figure 10 shows the influence of cutter position on chatter stability.

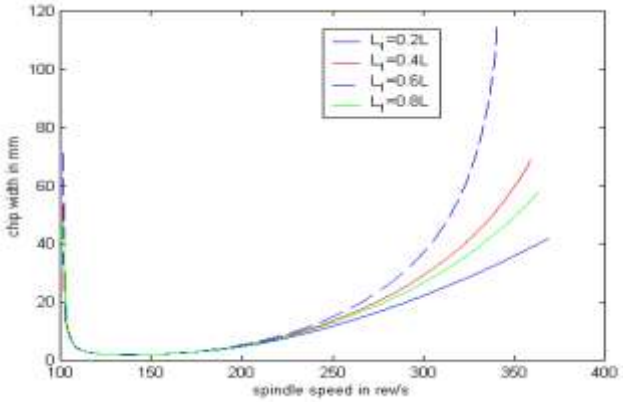

Fig.10 Effect of position of cutting in tailstock supported work-piece

Here a work-piece of 0.5m length and 0.03m radius is subjected to different tool forces at points: L_1=0.2L,0.4L, 0.6L and 0.8L. This analytical results suggest that the magnitude of the critical chip-width difference should decrease as the force is applied successively at 0.2, 0.4.0.6 and 0.8L respectively. As seen from the figure, critical chip width increases for some length (L_1=0.6L) as the tool moves towards the tailstock and then it decreases again. Here the cutting position (L_1) is accounted in terms of change in natural frequency of work-piece.

4.3 Effect of cutting tool dynamics

Fig.11 shows the chatter stability limits, when cutting tool stiffness k_1 changes from 0.5×10^7 N/m to 2×10^7 N/m at constant values of work-piece length L=0.5 m and radius r=0.035 m. From the diagram it is observed that as the tool becomes more flexible, critical chip width increases.

Journal of Engineering Technology (ISSN: 0747-9964)
Volume 6, Issue 2, July, 2017, PP.216-231

ORIGINAL ARTICLE

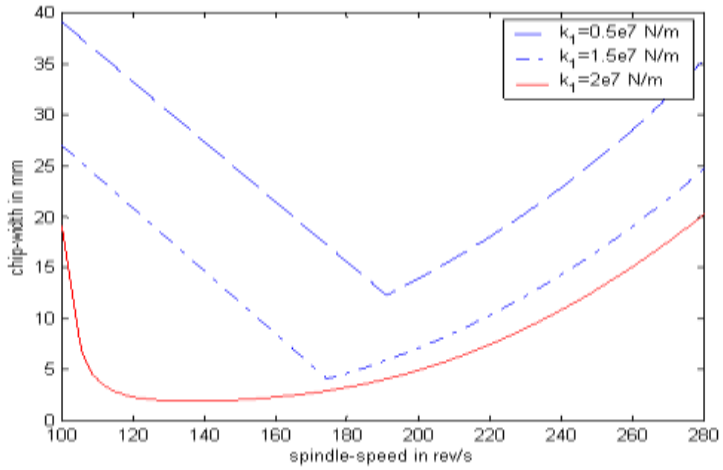

Fig.11 Effect of stiffness of cutting tool at high speeds (L = 0.5m, r = 0.035m)

Fig. 12 shows the effect of cutter-damping on the chatter stability for a cutter stiffness $k_1=0.5\times10^7$ N/m, along with work-piece dimensions: L=0.5m and r=0.035m. When damping increases in the cutter the stable depths of cut increase at the same spindle speeds.

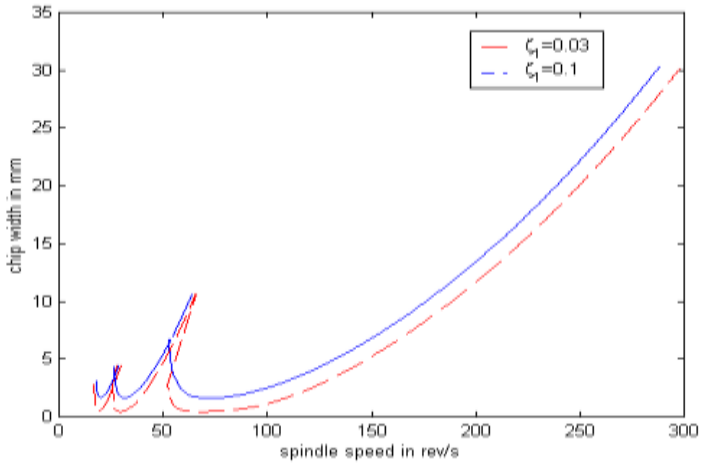

Fig.12 Variation of chip-thickness with spindle speeds as a function of damping ratio of tool(L = 0.5m, r = 0.035m)

4.4 Experimental Results

In order to validate the present model the experimental analysis is conducted as described in section 3. Various parameters of the cutting process and that of tool and work-piece are first obtained experimentally so as to draw the analytical lobe diagram from the proposed compliance model. The modal parameters namely, natural frequencies and damping ratios of work and tool are obtained from the conventional impact hammer test. Initially, the force and corresponding acceleration histories are directly recorded in the analyzer and the data is further employed to obtain the frequency response curves using a MATLAB program.

As seen from the amplitudes of the spectra, the fundamental natural frequency of the tool as 2560 Hz while the work-piece is around 612 Hz. For finding the experimental stability states, the predicted modal parameters are listed in Table 3.

Journal of Engineering Technology (ISSN: 0747-9964)
Volume 6, Issue 2, July, 2017, PP.216-231
ORIGINAL ARTICLE

Table 3. Major cutting conditions

Cutting Tool (carbide insert)	**Work-piece (AISI 1045 steel)**
Natural frequency $\lambda\omega_{n1}$=2560Hz	Natural frequency ω_{n2}=612 Hz
Damping ratio ξ_1=0.015	Damping ratio ξ_2=0.023
Stiffness $k_1=1.2\times10^7$ N/m	Stiffness $k_2=6.5\times10^6$ N/m

The cutting force coefficient (C) calculated from orthogonal data of AISI 1045 steel work-piece using shear stress, shear angle and friction angle with orthogonal transformations and it is found to be 700 MPa. Tool with coated-carbide insert employed during cutting has straight cutting edge without nose radius. In this test, AISI 1045 steel work-pieces are used. The metallurgical and mechanical properties of the workpiece material are presented in Table 4. The workpiece for the turning tests is a round bar of 60 mm of diameter and 250 mm of length.

Table 4 Metallurgical and Mechanical properties of AISI 1045 steel

Metallurgical properties		Mechanical properties	
Component	Wt. %	Property	Quantity
C	0.37-0.44	Hardness, Brinell	149
Fe	98.6-99	Tensile Strength, Ultimate	515 MPa
Mn	0.6-0.9	Modulus of Elasticity	200 Gpa
P	Max 0.04	Poisson's Ratio	0.29
S	Max 0.05	Shear Modulus	80 GPa

In such cases, X and Y components (thrust and feed force) would be relatively large. These suggest the patterns can be classified by monitoring the dynamic components of the three cutting forces. Altogether 9 different experiments are conducted at a constant feed rate of 0.246 mm/rev. Fig. 13 shows the dynamic components of three cutting forces in two different cutting states. As seen, the stable cutting is characterized by the lower amplitudes of dynamic component Fz and unstable process has wide amplitude variation in all force components.

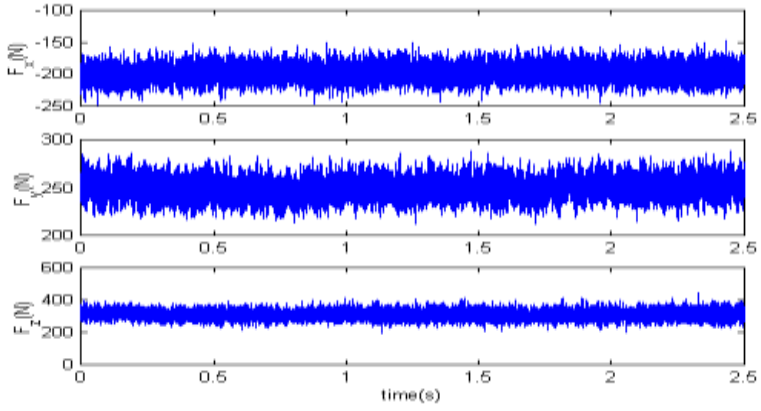

(a) Stable state (b=1.47 mm and N=770 rpm)

Journal of Engineering Technology (ISSN: 0747-9964)
Volume 6, Issue 2, July, 2017, PP.216-231

ORIGINAL ARTICLE

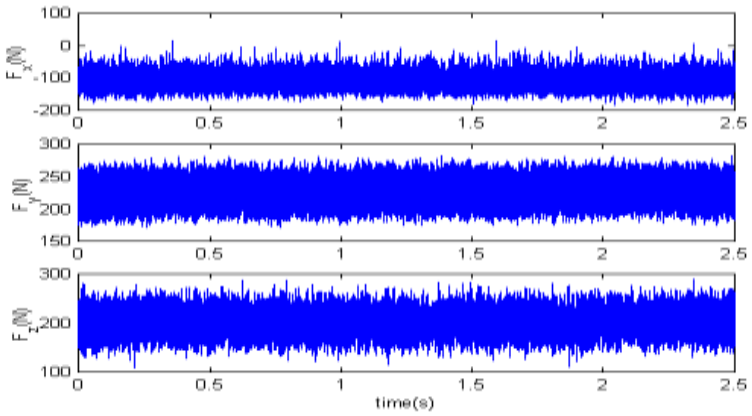

(b) Unstable state (b=1.58 mm and N=770 rpm)

Fig.13 Experimentally obtained dynamic cutting forces in 2 different states**.**

5. Conclusion

In this work while studying the compliance between the workpiece and cutting tool, the spring mass models have been employed and the relative deformations were considered in cutting force expressions. The methodology was presented with tailstock supported workpiece operated with cutting tool in orthogonal turning operation. Effect of cutting position, workpiece dimensions, cutter flexibility, and cutter damping on the dynamic stability have been presented with the proposed dynamic model. The deviations of stable depths of cut measured by present model and existing one-dimensional rigid workpiece model have been found to be in close agreement with available work in literature. The experimental chatter predictions have revealed that the proposed compliance model establishes the stable states accurately in rough turning operations.

References

[1] Boothroy. G, Knight. WA, "Chatter Vibration in Lathe tool-General characteristics of chatter vibration", Proc .Inst. Mech .Engg 1963 ; 77: 789-802.
[2] Astkhov. J, "Analysis of self excited vibrations in machine tool, Transactions of the ASME", Journal of Engineering for Industry 1964; 8: 123-131.
[3] Arnold. L, "The mechanism of tool vibration in the cutting of steel", Proceedings of the Institution of Mechanical Engineers 1965; 154: 261–276.
[4] Andrew. C, and Tobias. SAA, "Critical Comparison of two Current Theories of Machine Tool Chatter", International Journal of Machine Tool Design Research 1961; 1: 325-335.
[5] Gurney.JP, Tobias.SA, "A graphical analysis of regenerative machine tool instability", Transactions of the ASME Journal for Engineering Industry 1962; 103–112.
[6] Tlusty. J, Polacek. M, "The Stability of Machine Tool against Self-Excited Vibration in Machining", Proceedings of International Research in Production Engineering, Pittsburgh PA 1963; 465–474.
[7] Tlusty. JA, "A method of analysis of machine tool stability", International Journal of Machine Design and Research 1965 ; 6: 5–14.
[8] Tobias SA, Fishwick.W, "The chatter of lathe tools under orthogonal cutting conditions" Transactions of the American Society of Mechanical Engineers 1968; 80: 1079–1088.
[9] Tarng.YS, Young, Lee. B.Y, "An analytical model of chatter vibration in metal cutting", International Journal of Machine Tools and Manufacture 1994; 34: 183-197.
[10] Altintas.Y, Weck. M, "Chatter Stability of Metal Cutting and Grinding CIRP annals", Manufacturing Technology 2004 ;53: 619-642.
[11] Chen, Tsao.YM, "A stability analysis of turning a tailstock supported flexible work-piece", International Journal of Machine Tools and Manufacture 2006; 46: 18-25.
[12] Ganguli. A, Deraemaeke, Preumont.A, "Regenerative chatter reduction by active damping control", Journal of Sound and Vibration 2007; 300: 847-862.
[13] Chandiramani.NK, Pothala.T,"Dynamics of 2-dof regenerative chatter during turning", Journal of Sound and Vibration 2006; 290: 448–464.
[14] Dassanayake. AV, Suh.CS, "On nonlinear cutting response and tool chatter in turning operation", Communications in nonlinear science and numerical simulation, 2008; 13: 979-1001.
[15] Mei. C, Cherng. JG, Wang. Y, "Active control of regenerative chatter during metal cutting process", Trans ASME Journal of Manufacturing Science and Engineering, 2006; 128: 346-349.